

## Pyrolysis of the Caupi Bean Pod (*Vigna unguiculata*): Characterization of Biomass and Bio-Oil

Roberta M. Santos,<sup>a</sup> Diego F. Bispo,<sup>a</sup> Honnara S. Granja,<sup>a</sup> Eliana M. Sussuchi,<sup>b,a</sup>  
André Luis D. Ramos<sup>b</sup> and Lisiane S. Freitas<sup>b,\*a</sup>

<sup>a</sup>Departamento de Química, Universidade Federal de Sergipe (UFS),  
Campus Prof. José Aloísio de Campos, 49100-000 São Cristóvão-SE, Brazil

<sup>b</sup>Departamento de Engenharia Ambiental, Universidade Federal de Sergipe,  
Campus Prof. José Aloísio de Campos, 49100-000 São Cristóvão-SE, Brazil

The use of agricultural residues for the production of bio-oil is an important alternative to the use of fossil fuels. In this study, the Caupi bean pod (*Vigna unguiculata*) was characterized and used as biomass in the production of bio-oil. This biomass was evaluated in terms of physicochemical, morphological (scanning electron microscopy (SEM)), and thermal (thermogravimetric analysis (TGA), differential scanning calorimetry (DSC)) characterization, lignocellulosic composition, and pyrolysis processes. The pyrolysis was carried out in a stainless steel fixed-bed reactor (260 mm in length and 60 mm in diameter) under atmospheric nitrogen pressure. Pyrolysis was conducted at 550, 600, and 700 °C and N<sub>2</sub> gas flow of 2, 5, and 7 mL min<sup>-1</sup>. The chemical composition of the bio-oils was studied through CHN, TGA, Fourier-transform infrared spectroscopy (FTIR), and gas chromatography-mass spectrometry (GC-MS). The results confirmed the bean pod's potential in the thermochemical process. The thermogravimetric analyses demonstrate that there can be a relationship between the components of the principal biomass (cellulose, hemicellulose, and lignin) and the compounds present in the bio-oil. The obtained bio-oils represent bio-products that are rich in compounds of several chemical classes with relevant commercial value such as acids (palmitic, linoleic, oleic, and stearic), alcohols (ethylene glycol), sugars (levoglucosan), and phenols (guaiacol, catechol, phenol, and pyrocatechol).

**Keywords:** residue, bean pod, pyrolysis, bio-oil

### Introduction

The biomass from agricultural waste is a promising source of substitutes of conventional fuels because of their high energy potential and high carbon content.<sup>1</sup> Among the various types of agricultural waste, that from bean crops (represented by straw and pods) is highlighted<sup>2</sup> because it is produced in large amounts as the result of grain processing.<sup>3</sup> Because these residues require a significant amount of time to be naturally degraded and absorbed in the soil, several studies investigated the reuse of these types of biomass in the generation of products with aggregated value.<sup>4</sup>

Agricultural residues that are classified as the lignocellulosic biomass type are mainly composed of cellulose, hemicellulose, and lignin, and have high energy content. These raw materials can be converted into energy

products through thermochemical conversion methods, such as pyrolysis, which is one of the most efficient technologies for producing energy, fuels, and high-value chemicals.<sup>5</sup> Hydrodeoxygenation (HDO) can be used for the transformation of phenols originated from pyrolysis in cyclohexane and other hydrocarbons for fuel generation.<sup>6</sup> Pyrolysis is the thermal degradation of organic material in the absence of oxygen at relatively low temperatures (400-900 °C) that results in the formation of the following products: solid (biochar), liquid (bio-oil), and biogas (CO, CO<sub>2</sub>, H<sub>2</sub>, H<sub>2</sub>O, and CH<sub>4</sub>).<sup>7</sup>

The utilization of the biomass from agricultural residues in the pyrolysis process has been extensively explored. Mythili *et al.*<sup>8</sup> selected 25 types of agricultural wastes and pyrolyzed them at 450 °C in a fixed bed reactor to produce bio-oils. The maximum bio-oil yield was obtained from the Pinfed computer paper (45%) and the minimum from residues of *Parthenium hysterophorus* (6.33%); this difference is related to the amount of lignin-cellulose

\*e-mail: lisiane.ufs@gmail.com, lisiane\_santos\_freitas@yahoo.com.br  
This article is part of the Special Issue Brazilian Women in Chemistry.

present in the biomass. Pyrolysis at lower temperatures is facilitated in biomasses with a high percentage of cellulose. The results confirmed that the volatile material and cellulose content significantly influenced the bio-oil yield, which can be used as fuel in boilers and diesel engines for power generation as a substitute for fossil fuels. Hawash *et al.*,<sup>9</sup> studied the pyrolysis of seven different agricultural residues in a tubular furnace reactor at 500 °C for 15 min. The produced bio-oil and biochar were studied with the purpose of determining their chemical composition and quality. In that study, the highest percentage of bio-oil and calorific power were obtained from *Jatropha* seeds (24.29 wt.% and 38 MJ kg<sup>-1</sup>, respectively) while residues from *Jatropha* cake and *Jatropha* hulls generated lower percentages of bio-oils and average calorific power of 32.15 and 27.87 MJ kg<sup>-1</sup>, respectively.

In 2014, the production of beans (*Vigna unguiculata*) in Brazil was 482.665 tons, ranking fourth in the world behind Burkina Faso (571 mil tons).<sup>10</sup> In the production of dry mass from Caupi, between 24.5 and 26.2% are derived from beans and 73.8-75.5% from stems, leaves, flowers, and pods.<sup>11</sup> The bean pod (*Vigna unguiculata*) residue is generated in large quantities in agriculture and is generally used as animal feed or burned, causing major effects on soils and air.

This study investigated the influence of operational conditions on the yield of bio-oils obtained from the pyrolysis of Caupi bean pods and the characterization of the obtained bio-oil. The biomass was analyzed using physicochemical methods, elemental analyses, thermogravimetric analysis (TGA), and Fourier-transformed infrared spectroscopy (FTIR). The bio-oil was characterized by gas chromatography mass spectrometry (GC-MS).

## Experimental

### Raw material

Caupi bean pods were purchased from a local market in Aracaju-Sergipe, Brazil, and used as biomass for all pyrolysis experiments. The collected samples were washed repeatedly with distilled water to remove dust and dirt and dried in an oven at 60 °C for 24 h. The dried material was subsequently milled and sieved to produce samples with grain diameters between 0.25 and 0.42 mm. These samples were stored in a glass bottle before pyrolysis.

### Characterization of biomass

#### Physicochemical and elemental analyses

The moisture content (ASTM D 3173-87)<sup>12</sup> was determined in the bean pod by heating samples in a hot

air oven at 103 ± 2 °C up to reaching constant weight. Ash content (ASTM D 3174-89)<sup>13</sup> was determined by heating samples at 750 °C for 6 h. The volatile matter (ASTM D 1762-84)<sup>14</sup> was calculated by measuring the weight loss in the dried sample (placed in a muffle furnace at 850 °C for 2 min). The carbon, hydrogen, and nitrogen contents of the dried biomass samples were determined using the LECO CHN-628 equipment; the results were treated in the CHN628 software version 1.3. The equipment was operated with helium (99.995%) and oxygen (99.99%), with the furnace temperature at 950 °C and the afterburning temperature at 850 °C. Other parameters were adjusted to obtain increased sensibility. The equipment was calibrated with the ethylenediaminetetraacetic acid (EDTA) standard (41.0% C, 5.5% H, and 9.5% N) using mass ranging between 10 and 200 mg. The standard and samples were analyzed using 100 mg for organic samples and 200 mg for inorganic samples in a tin foil. Oxygen was determined by the difference expressed as O (wt.%) = 100 - (C + H + N). The highest heating value (HHV) was determined using the correlation proposed by Sheng and Azevedo<sup>15</sup> and based on the composition of the main elements, as shown below:

$$\text{HHV (MJ kg}^{-1}\text{)} = -1.3675 + (0.3137 \times \text{C}) + (0.7009 \times \text{H}) + (0.0318 \times \text{O}) \quad (1)$$

where C, H, and O are the weight percentages of carbon, hydrogen, and oxygen, respectively. The protein content was measured according to the method reported by Hames *et al.*<sup>16</sup> Cellulose, hemicelluloses, and lignin were measured according to the VanSoest's method.<sup>17</sup>

### Thermal, morphological, and functional analyses

The thermogravimetric analysis (TGA) analyses of raw bean pods were applied to determine the thermal degradation behavior of the biomass by its weight loss with increasing temperatures using the Shimadzu DTG-60H instrument. These tests were conducted using 5 mg samples at a heating rate of 10 °C min<sup>-1</sup> within the temperature range of 25-1000 °C and under an N<sub>2</sub> atmosphere of 100 mL min<sup>-1</sup>.

The differential scanning calorimetry (DSC) analysis was carried out in the Shimadzu DSC-60 instrument; the curve was obtained with a raw mass of 3.0 ± 0.5 mg, a heating rate of 20 °C min<sup>-1</sup> within the range of 30-600 °C, and under N<sub>2</sub> atmosphere of 100 mL min<sup>-1</sup>. The morphological analyses were performed by scanning electron microscopy (SEM) in the Aspex-PSEM Explorer and FEI QUANTA 200F devices. Before analyses, samples were metalized with a layer of 5 nm gold. The FTIR

spectra were collected on a Varian (model 640-IR) FTIR spectrophotometer with the sample powder diluted in KBr over the range of 400–4000  $\text{cm}^{-1}$ , resolution of 4  $\text{cm}^{-1}$ , and 32 scans.

### Pyrolysis experiments

These experiments were conducted on a laboratory scale pyrolysis pilot plant (Figure 1). The pyrolysis was carried out in a stainless steel fixed-bed reactor (260 mm in length and 60 mm in diameter) under atmospheric nitrogen pressure. Volatile compounds were collected in Teflon tubes and refrigerated in a thermostatic bath (Microquímica Equipments LTDA, model MQBTC99-20) at approximately 10 °C. The variables were set as 550, 600, and 700 °C, sample weight of 8 g, and  $\text{N}_2$  gas flow of 2, 5, and 7  $\text{mL min}^{-1}$ . The pyrolysis time of 50 min (after the reactor reached the pyrolysis temperature) and constant heating rate of 30  $^\circ\text{C min}^{-1}$  was used in all experiments. The bio-oil was separated from the aqueous fraction and analyzed by chromatography as described in Onorevoli *et al.*<sup>18</sup> The pyrolysis process resulted in solid, liquid (bio-oil + water), and gas products.

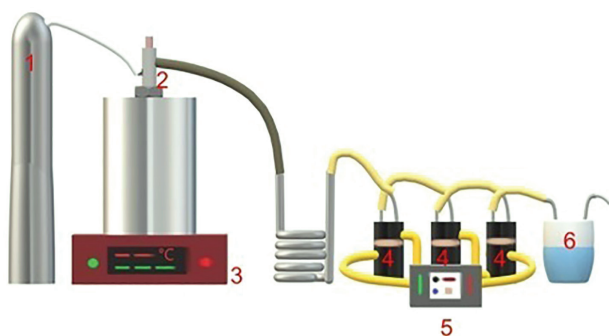


**Figure 1.** Schematic diagram of the pyrolysis set-up: 1: nitrogen cylinder; 2: reactor; 3: furnace; 4: collector tubes; 5: thermostatic bath; 6: gas outlet.

### Analyses of the bio-oil produced from the pyrolysis

The chemical composition of the bio-oil was evaluated by elemental and thermogravimetric analyses and infrared spectrometry using the methodologies described above. The bio-oil samples were derivatized with bis(trimethylsilyl), trifluoroacetamide (BSTFA), and trimethylchlorosilane (TMCS) to volatile trimethylsilyl ester derivatives,<sup>19</sup> and analyzed by the GC-MS (Shimadzu QP2010 Plus, Shimadzu, Tokyo, Japan) equipped with an AOC20i autoinjector (split/splitless). A ZB-5MS column (60 m  $\times$  0.25 mm internal diameter (i.d.)  $\times$  0.25  $\mu\text{m}$  thick film) was used for separation. An isothermal oven program was set initially at 90 °C for 2 min and raised to 160 °C at the rate of 2  $^\circ\text{C min}^{-1}$ , and subsequently set as the final

temperature at 280 °C at the rate of 15  $^\circ\text{C min}^{-1}$  for 10 min. The temperatures in the injector and detector were 280 and 300 °C, respectively. The injection was performed in the split mode (1:20), and the flow of carrier gas (He, ultra-pure, White Martins S.A., Aracaju, Brazil) was 1.0  $\text{mL min}^{-1}$ . The chemical components were tentatively identified by comparing the retention time and major mass fragments in the detectable peaks with those of authentic standards from the NIST-05 mass spectral library (with the NIST and Wiley libraries).

## Results and Discussion

### Characteristics of the raw material

#### Proximate and ultimate analyses

The proximate and ultimate analysis of the bean pods were estimated to evaluate the main constituents of the biomass, which directly influence the characteristics of final pyrolysis products. The estimated moisture content for this type of agricultural residue (8.88%) was considered ideal because the pyrolysis process generally requires biomasses with a moisture content of less than 10%, when dry, to guarantee its quality and facilitate heat transfer, processing, and storage of final conversion products.<sup>20</sup> Ashes are the solid waste from the complete combustion of biomass in the form of silicon oxide, aluminum, iron, calcium, magnesium, manganese, titanium, phosphorus, sulfur, sodium, and potassium. The presence of these elements may reduce the pyrolysis efficiency causing corrosion, slag, and contamination in thermochemical processes.<sup>21</sup> Conversely, this material has a catalytic effect during bioconversion because it is present in the biomass in the form of cations, influencing both the pyrolysis process and distribution of pyrolysis products.<sup>22</sup> The bean pod sample showed low ash content (4.38%) when compared with other biomasses such as straw and rice husk residues (15.00 and 15.14%, respectively).<sup>23</sup> This low ash content reflects in its properties, for example, with superior calorific power. The use of biomass with a high content of inorganic compounds in pyrolysis favors decreased bio-oil yields and increased biochar production, which has catalytic potential in thermal conversion technologies.<sup>23</sup>

The content of volatile material corresponds to condensable vapors and non-condensable gases, released from the biomass after heating, at percentages ranging from 64 to 98%.<sup>24</sup> The high content of volatiles in the bean pod (86.74%) defines it as a material rich in volatile organic compounds.

The elemental analysis evaluates the bioconversion potential of the biomass to be used in the pyrolysis

process. The elemental content of C, H, N, and O showed that the bean pod contains high proportions of oxygen (46.36%) and carbon (42.01%). Generally, biomasses from agricultural residues present percentages of around 45% of carbon and above 50% of oxygen due to their high constitution with holocellulose.<sup>25</sup> The hydrogen content measured in the bean pod (5.89%) was close to that found in residues of corn straw (4.7-6.3%) and corn cob (5.0-7.4%).<sup>24</sup> The H/C and O/C atomic ratios are associated with the material's degree of condensation or aromaticity. The higher H/C ratio (1.67) can be explained by the greater amount of aromatic groups, while the O/C ratio (0.83) indicates the content of oxygen groups in the material. The nitrogen content contributes to the emissions of NO<sub>x</sub> gases, which are pollutants and affects the quality of the pyrolysis liquid products. However, it is also associated with the protein content present in the material. The low nitrogen content value obtained in the bean pod (1.36%) was considered satisfactory, and based on this value, the protein content (8.50%) was estimated using a nitrogen-protein conversion factor indicated for all types of biomasses (6.25).<sup>16</sup> These results are similar to those found in bean peel (1.35% nitrogen content and 8.44% protein content) and higher than that found in green beanstalk and peel (0.78% nitrogen content and 4.87% protein content).<sup>26</sup> The energetic content available in the biomass in the form of heat, that is, the superior calorific value, was calculated from the elementary results using the equation proposed by Sheng and Azevedo,<sup>15</sup> and determined as 17.55 MJ kg<sup>-1</sup>. This value was lower than that determined for sesame residues (21.04 MJ kg<sup>-1</sup>) and soybean residues (19.26 MJ kg<sup>-1</sup>).<sup>26</sup> The low calorific value of the biomass is relative and associated with the oxygen content, that is, the higher the percentage of this element, the lower the calorific value because they release less heat during combustion. This is demonstrated in the results presented by Park *et al.*,<sup>27</sup> when analyzing garlic and pepper stems. Both materials presented high oxygen percentages (47.84 and 46.42%, respectively) and, consequently, low calorific value (18.36 and 19.39 MJ kg<sup>-1</sup>, respectively).

#### Lignocellulosic components

The main constituents identified in the bean pods were cellulose (29.97%), hemicellulose (24.33%), lignin (7.31%), extractives and minerals (38.39%), which are in agreement with data reported in the literature;<sup>28</sup> the cellulose content was close to that of rice husk (30.42%) and inferior to that in corn husk (43.97%), and the hemicellulose and lignin contents were lower than the

values reported in those biomasses (28.03 and 28.94%, and 36.02 and 21.82%, respectively).<sup>28</sup> Ho *et al.*,<sup>29</sup> reported the chemical composition of different agricultural residues, which ranged from 33-46% for cellulose, 18-35% for hemicellulose, and 7-29% for lignin. The proportion of each organic component varies depending on the type of biomass, crop location, and harvest time. In the pyrolysis process, these components also exhibit a strong influence on the characteristics of the paths of chemical reactions and consequently in the products, i.e., higher amounts of cellulose and hemicellulose contribute to the yield of bio-oil, while lignin, in addition to interfering with the biochar yield, it can increase viscosity and form compounds with a high molecular mass in the bio-oil.<sup>30</sup> Thus, the low lignin content in the evaluated material can be considered positive regarding pyrolysis and bio-oil yield. In addition to influencing the yields of products, the influence of some compounds present in the bio-oils is also observed. For example, sugars are derived from the depolymerization of holocellulose, furans are formed when cellulose is subjected to medium and high temperatures, long-chain fatty acids are formed from the desacetylation of hemicellulose and holocellulose fragmentation, and phenolic compounds are formed through demethoxylation reactions and dimethylation and alkylation of the lignin structure.<sup>31</sup>

#### Thermogravimetric analyses

The thermogravimetric analysis was used in this study aiming at optimizing the pyrolysis' conditions because this allows the evaluation of mass-loss rates that occur in biomasses when temperatures are varied. Figure 2 shows the TGA and derivative thermogravimetry (DTG) curves for the bean pod. The DTG curve clearly shows three zones of mass loss, which can be explained by the sample's degradation involving various types of competitive and/or consecutive reactions; the maximum decomposition event was at 400 °C with a total mass loss of 61.75%. However, in the range of 400 to 600 °C, the decomposition occurs with approximately 8.88% mass loss.

The first decomposition zone between 30 and 120 °C corresponds to the loss of moisture and low molecular mass volatile compounds (8.10% mass loss). The second zone between 120 and 272 °C is associated with the hemicellulose depolymerization reaction and degradation of part of the cellulose and bound water (21.54% mass loss). The third zone between 272 and 400 °C corresponds to the cellulose decomposition range (32.11% mass loss). The decomposition of the remaining lignin, which starts at low temperatures and increases up to approximately 1000 °C,

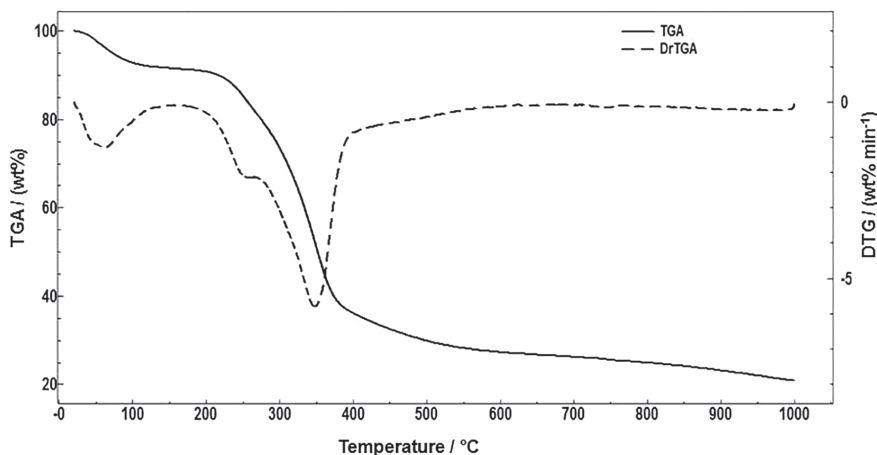


**Figure 2.** TGA/DTG curves of bean pod biomass.

results in approximately 21.00% of carbon residue and inorganics. Hemicellulose is composed of monosaccharides (pentoses) consisting mainly of anhydroxylose units; their decomposition starts at low temperatures ranging from 220 to 315 °C. Cellulose, being a crystalline polymer of high molecular mass, decomposes at high temperatures ranging from 315 to 400 °C. The decomposition of residual lignin and other components occurred at over 400 °C. Lignins are composed of three types of phenylpropane units with high molecular mass, and therefore, of higher thermal stability when compared to hemicellulose and cellulose, which consequently leads it to decompose at a slower rate.<sup>32,33</sup>

#### Differential scanning calorimetry analyses

In the differential scanning calorimetry, it is possible to evaluate the thermal stability of the material based on the occurrence of exothermic or endothermic reactions. As with thermogravimetric curves, those for DSC also showed

regions of exothermic reactions that provide clues about the sample thermal degradation behavior (Figure 3).

The comparison of the DSC and TGA/DTG curves for the bean pod showed that an endothermic event started at room temperature and went up to 100 °C at an energy absorption  $T_{max}$  of 86 °C, coinciding with the first mass loss in the TGA/DTG analysis. This first peak corresponds to the material's dehydration and the initial heating for the evaporation of slightly volatile compounds. The second stage, characterized by an exothermic event of 100-500 °C and  $T_{maximum}$  energy release at 430 °C, coincides with the second mass loss event in the thermogravimetric analysis, which refers to the organic matter degradation present in the material corresponding to the lignocellulosic fractions. According to Kok and Ozgur,<sup>34</sup> degradation temperatures depend on the biomass and heating rate. Similar results have been reported by Mishra<sup>35</sup> when studying the thermal behavior of sawdust biomass. The curves showed two peaks related to the evaporation of water molecules and

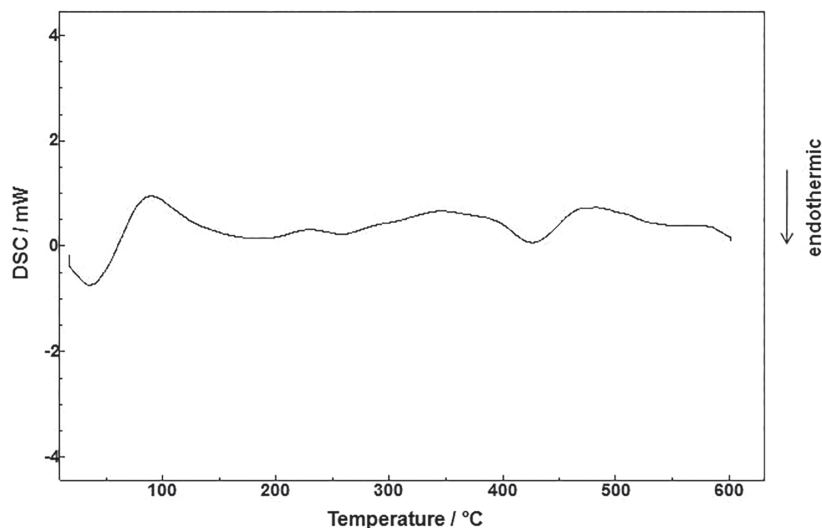


**Figure 3.** DSC curve of bean pod biomass samples.

the degradation of cellulose and hemicellulose compounds, respectively.

#### FTIR analyses

Figure 4 shows the infrared spectrum of the bean pod sample. The FTIR analysis was used to evaluate the chemical structure of the biomass principal components. The structure showed the presence of cellulose, hemicellulose, and lignin in the biomass.

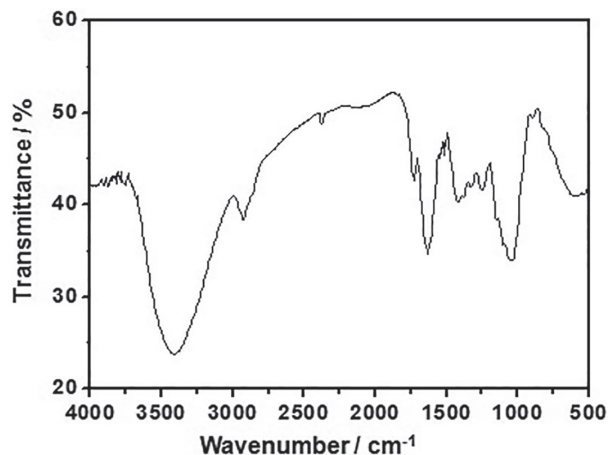


Figure 4. FTIR spectrum of bean pod.

The sample showed a very strong and intense absorption band at  $3350\text{ cm}^{-1}$  corresponding to the OH vibration stretch of intramolecular hydrogen bonds from the cellulose molecule.<sup>36</sup> The  $2910\text{ cm}^{-1}$  band was attributed to the symmetrical and asymmetrical  $\text{CH}_2$  and  $\text{CH}_3$  stretch of alkanes, alkenes and cellulose. The vibration stretch at  $1736$  and  $1240\text{ cm}^{-1}$  may be associated with  $\text{C}=\text{O}$  and  $\text{CO}$  bonds of alkyl esters units of acetyl groups present in hemicellulose and/or bonds between hemicellulose

and lignin.<sup>32</sup> At  $1631\text{ cm}^{-1}$ , an absorption band ( $\text{C}=\text{O}$ ) is suggested with vibration stretch characteristic of aromatics that are present in lignin. The absorption band at  $1420\text{ cm}^{-1}$  refers to the  $\text{C}-\text{H}$  deformation in the methoxy groups of lignin. The band at  $1050\text{ cm}^{-1}$  may be evidenced by acid groups and esters. However, it may also be associated with the  $\text{C}-\text{O}-\text{H}$  stretching of primary and secondary alcohols. In the  $920-1190\text{ cm}^{-1}$  region, the absorption band corresponds to the  $\text{C}-\text{O}$  and  $\text{C}-\text{C}$  bonds and the structural deformations of the  $\text{CH}_2\text{OH}$  ring.<sup>37</sup>

#### Scanning electron microscopy analyses

Micrographs of the sample *in natura* are presented in Figure 5. The images show that the bean pod presents a slightly damaged surface due to the milling and sieving process. However, it is still possible to observe the presence of elongated fibers that are typical of lignocellulosic material, besides grooves, roughness, and small superficial pores.<sup>38</sup> Similar observations are reported by Sindhu *et al.*,<sup>36</sup> when evaluating the surface of sugarcane bagasse presenting a rigid and compact structure.

#### Bio-oil characterization

##### Influence of pyrolysis conditions on the bio-oil

The chemical profile of bio-oils varies with the conditions of processing, including temperature and gas flow.<sup>39</sup> However, in this study, the temperature variation and gas flow did not significantly influence the characteristics of the bean pod bio-oils. According to Guedes *et al.*,<sup>40</sup> it is expected that the quality of bio-oils is influenced by temperature because bio-oils obtained at low temperatures are mainly formed by alkenes, alkanes, long-chain fatty acids, esters, nitriles, and amides, while high temperatures

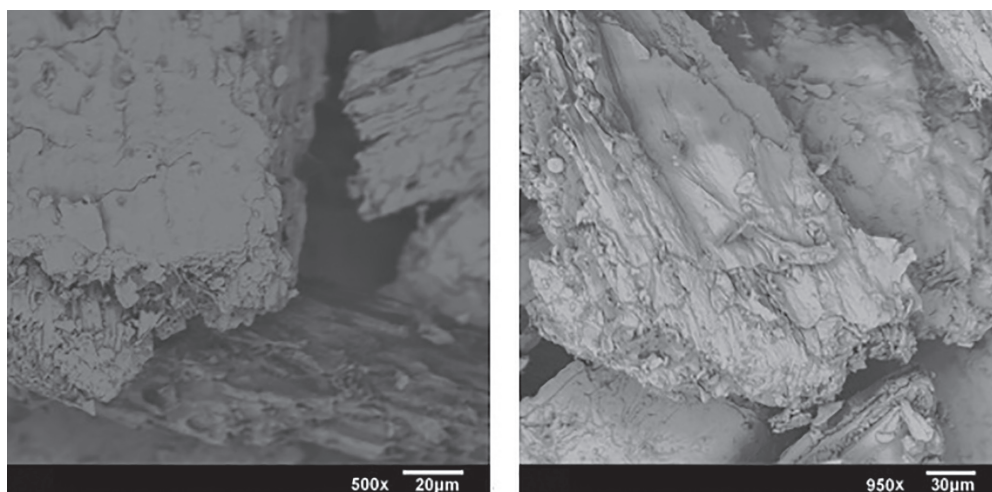


Figure 5. Scanning electron micrographs of bean pod.

favor the cracking of aliphatic species and formation of aromatics (in general phenols), resulting in lower ratios of H/C in the obtained bio-oils.

Gas flow rate ( $N_2$ ) is another parameter that affects compounds in bio-oils by influencing the time residence of vapors pyrolysis inside the reactor. High-gas flow rates provide the formation of gas because volatiles do not go through condensation and repolymerization effectively; conversely, vapors stay longer in the pyrolytic zone under low-gas flow rates, and the interaction between compounds is more evident, favoring greater cracking.<sup>41</sup>

#### Elemental analysis of the bio-oil

The pyrolysis experiments (I, II, III, IV, and V) were performed under different conditions, and the bio-oils obtained presented similar elementary compositions (Table 1).

The percentage of carbon, hydrogen, and nitrogen were higher than those in the raw material, which means that the obtained bio-oils are more energetic. The oxygen percentage of the bean pod bio-oil was lower than that found in the bio-oil from the pyrolysis of sugarcane leaves (33.32%).<sup>42</sup> According to the literature,<sup>42</sup> the amount of oxygen in bio-oils from lignocellulosic material varies from 35 to 40% and is distributed in compounds classes of carboxylic acids, hydroxyaldehydes, hydroxyketones, sugars, and phenolics. In fact, the presence of these oxygenated compounds in bean pod bio-oils was confirmed by the GC-MS analysis. High oxygen content contributes to low pH values making bio-oils corrosive and unstable during transport and storage; in these conditions, bio-oils cannot be used as biofuels but can be sources of value-added chemicals.<sup>43</sup> The results showed that the high carbon content resulted in the increase of the bio-oils' superior calorific value (HHV) and reduction of the H/C molar ratio compared to the raw material. The calorific value of the bean pod bio-oil was higher than that of other bio-oils produced from the pyrolysis

of other biomasses such as corn flour (17.51 MJ kg<sup>-1</sup>) and apricot kernel (22.72 MJ kg<sup>-1</sup>).<sup>44</sup> The comparison between the heating value- of the bio-oils with those of some fossil fuels showed that they were lower than that of diesel (45.4 MJ kg<sup>-1</sup>) and gasoline (47.3 MJ kg<sup>-1</sup>), which can be attributed to the bio-oils high content of degradation products that contain oxygen or condensed water. This contributes to lowering the ignition and emission temperatures of this biofuel as well as increasing its flowability. On the other hand, conventional fuels have high calorific values because they consist of high carbon and hydrogen contents and low oxygen contents.<sup>45</sup>

#### Thermogravimetric analyses of the bio-oil

Figure 6 shows the TGA/DTG curves of the bean pod bio-oil obtained in different pyrolysis conditions. The analysis allows determining the nature of volatile and semi-volatile compounds formed during the pyrolysis process.

The profiles of the TGA curves for samples I, II, and V were similar, demonstrating the high thermal stability of the liquid product. In the temperature range of 30-150 °C, the mass loss percentages of these bio-oils were approximately 33.77, 29.85, and 30.48%, respectively, occurring mainly because of the release of water and volatiles. According to Fan *et al.*,<sup>46</sup> compounds that are present in the TGA curve at temperatures lower than 250 °C may be derived from unstable esters and carboxylic acids that will be transformed to produce CO<sub>2</sub>. In the 30-150 °C temperature range, bio-oils III and IV presented lower mass loss percentages (15.81 and 25.27%, respectively), which can be explained by the presence of less volatile compounds in the material. After this event, the degradation of bio-oils continued until reaching 400 °C, totaling a mass loss of around 80%. The mass losses in all bio-oils ranged from 4.81 to 8.11% at temperatures above 400 °C. The DTG curves clearly showed a mass loss event in the temperature range of 150-350 °C in all bio-oils. In this region, the highest

**Table 1.** Bio-oil elemental analyses and HHV

Experiment	Pyrolysis conditions		Carbon / %	Hydrogen / %	Nitrogen / %	Oxygen / %	H/C	HHV / (MJ kg <sup>-1</sup> )
	Temperature / °C	Flow / (mL min <sup>-1</sup> )						
I	550	5	60.29	8.31	1.30	25.71	1.64	24.19
II	600	2	61.88	8.13	2.03	23.58	1.57	24.49
III	600	5	60.19	7.90	2.46	23.85	1.56	24.00
IV	600	7	62.53n	8.26	1.69	24.77	1.57	24.91
V	700	7	62.70	8.14	1.74	23.04	1.54	24.74

HHV: highest heating value.

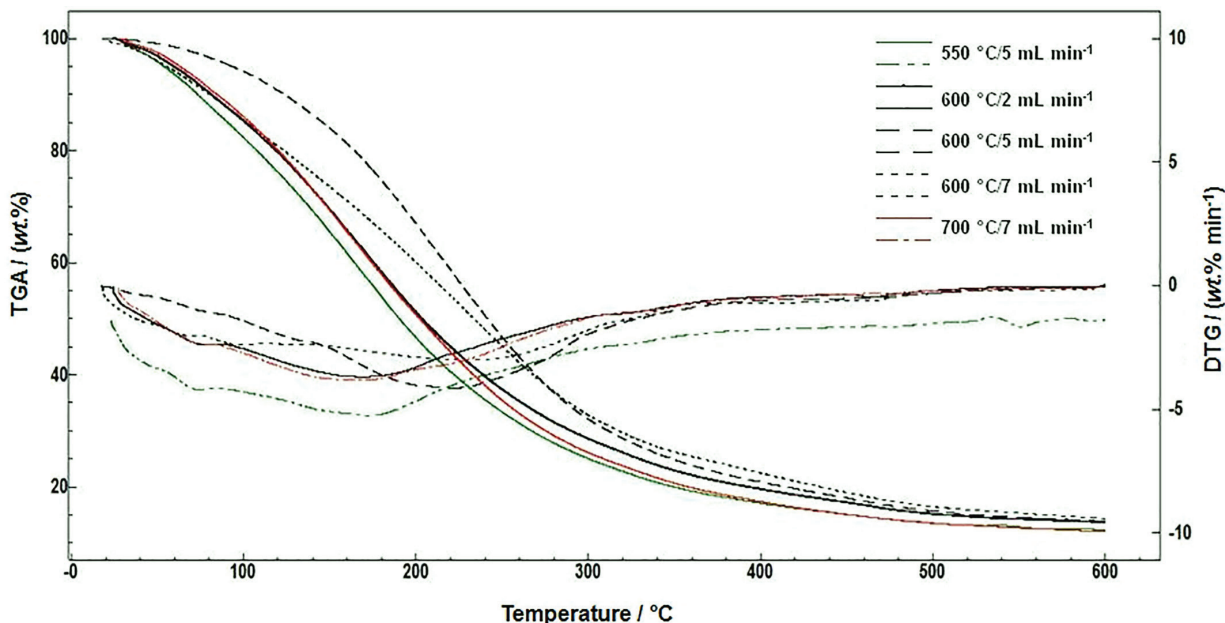


Figure 6. TGA curves bio-oil of bean pod samples.

percentages of mass loss were in experiments III and V (59.21 and 48.74%, respectively) while the lowest mass loss occurred in experiment I (45.56%). The higher mass loss in experiments III and V in relation to experiment I can be explained by higher temperatures; a greater degradation of biomass compounds occurs at higher temperatures during pyrolysis, and therefore, the bio-oil produced contains more volatile compounds and less high molecular weight compounds in its constitution. Conversely, the mass loss was lower at low temperatures, favoring the polymerization of bio-oil components.<sup>47</sup> The residual carbon content ranged from 12.14% in experiment V to 15.55% in experiment IV. The lower the residual carbon content, the lower the amount of aromatic molecules, which suggests an increased degradation of the bio-oil.

In general, it can be said that the pyrolysis conditions (temperature and inert gas flow) did not significantly change the TGA curves, especially mass loss temperatures with small changes in the percentage of mass loss in each band.

#### FTIR spectroscopy of the bio-oil

The Fourier transform infrared (FTIR) spectra of the bio-oils are shown in Figure 7. The spectra of the bio-oils samples showed similar profiles, however, with different bands intensities.

The absorption bands between 3000 and 3700  $\text{cm}^{-1}$  correspond to the O–H vibration stretch, indicating the presence of phenol, alcohol, and carboxylic acids, in addition to the humidity. The C–H vibration stretch at 2800–3000  $\text{cm}^{-1}$  and C–H deformations between

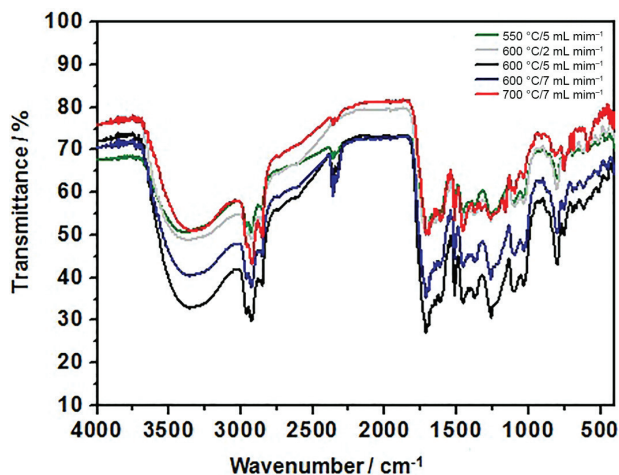


Figure 7. FTIR spectrums of bio-oils.

1350–1475- $\text{cm}^{-1}$  suggest the presence of hydrocarbons. The C=O absorption in the 1650–1750  $\text{cm}^{-1}$  region suggests the presence of aldehydes, ketones, esters, or acids; the C=C stretch at 1575–1675  $\text{cm}^{-1}$  indicates the presence of alkenes and aromatics; and the absorption peaks between 900–1300  $\text{cm}^{-1}$  shows the presence of primary, secondary, and tertiary alcohols. The absorption peaks between 650–800  $\text{cm}^{-1}$  and 1420–1610  $\text{cm}^{-1}$  indicate substituted aromatic groups. The different absorption bands identified in the bio-oils samples are correlated with the contents of cellulose, hemicellulose, and lignin present in the bean pod *in natura*.<sup>48</sup> These bands present similarities with those determined by Biswas *et al.*,<sup>23</sup> when studying the composition of bio-oils obtained from the pyrolysis of corn cobs, wheat straw, rice straw, and rice husk.

## Gas chromatography-mass spectrometry (GC-MS) of the bio-oil

The bio-oil is composed of numerous organic compounds belonging to different chemical classes and originated from the conversion of the bean pod biomass under different pyrolysis conditions; total ion current chromatogram (TICCs) are represented Figure S1 in the Supplementary Information section. The qualitative analysis and identification of compounds were performed considering compounds with an area greater than 10% and similarity greater than 85% when comparing the mass spectra using the Nist 05 and Wiley libraries. Figure 8 presents the distribution graph of compounds present in the bio-oils according to chemical classes.

The data analysis showed that the major components were phenols (> 50%) followed by acids (> 20%); however, nitrogen compounds, sugars, alcohols, aldehydes, ketones, and others were also identified. In general, the percentage of phenol compounds increase with increased temperatures, probably as the result of increased degradation of lignin, especially at temperatures above 500 °C. The graph showed that the increase from 550 °C (exp. I) to 600 °C (exp. IV), and 700 °C (exp. V), favored the increase in compounds belonging to the class of phenols. This fact results from the increased degradation of lignin and secondary degradation of compounds from oils and cellulose, which begin forming low molecular weight compounds favoring the formation of biogas. Nitrogen compounds (3.2-6.3%), sugars (0-9.6%), and others (11.7-14.7%) were determined with percentage areas of less than 15%. In flows over 5 mL min<sup>-1</sup> and temperature above 600 °C there is a decrease in sugar concentration due to the cellulose instability.

The phenols present in the bio-oils are usually directly related to the thermal decomposition of lignin that occurs at high temperatures during pyrolysis through demethoxylation, demethylation, and alkylation of this macromolecule.<sup>49</sup> However, a bio-oil rich in phenol can also be formed from interactions between cellulose and lignin. According to Hosoya *et al.*,<sup>50</sup> interactions between cellulose-hemicellulose molecules do not occur significantly during biomass pyrolysis while cellulose-lignin interactions are more evident with lignin inhibiting levoglucosan formation and cellulose improving the formation of products derived from lignin.

Although the percentage of bean pod lignin was relatively low (7.31%), the phenolic compounds in the bio-oil were identified as the majority, indicating that these compounds were not only formed by lignin pyrolysis but also by the secondary reactions of products derived from cellulose.<sup>51</sup> Phenols represented most of the identified organic compounds. The same phenolic compounds (19 compounds) were found in all tested pyrolysis experimental conditions. No apparent differences were observed between the area percentages of the compounds in experiments I and III in which the temperature was varied and the gas flow maintained. On the other hand, experiments IV and V showed an increase of approximately 10% in the area percentage, which can be explained by the gas flow rate and higher temperature, favoring demethoxylation, demethylation, and alkylation reactions, increasing catechol-cresol compounds and decreasing guaiacol compounds.<sup>52</sup> In experiments II and III, the gas flow variation did not significantly influence the percentage area of compounds.

The main phenolic compounds identified in the bean pod bio-oils are presented in Figure 9. The changes in pyrolysis

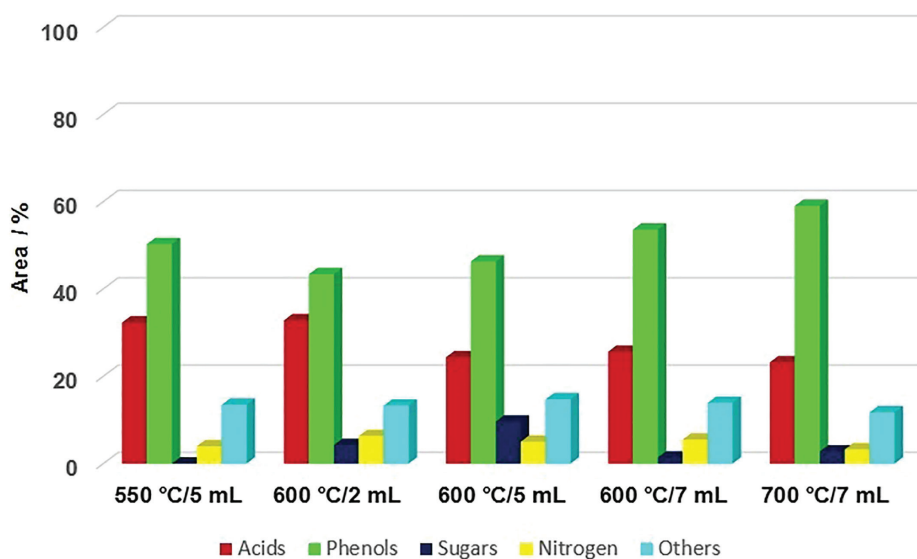


**Figure 8.** Distribution of compounds in bio-oil samples produced from pyrolysis bean pod under different experimental conditions.

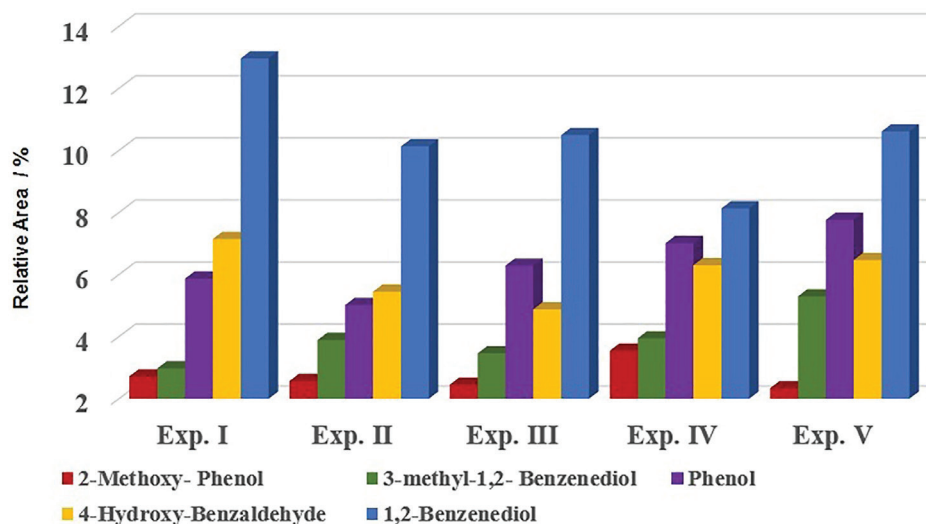


Figure 9. Phenolic compounds detected in bio-oils from bean pod.

experimental conditions influenced the percentage area relative to each compound.

In general, the increase in flow and temperature from 550 °C (exp. I) to 700 °C (exp. V) provided the increase in the percentage area of phenol and 3-methyl-1,2-benzenediol (3 methyl catechol). Higher temperatures favor reactions of demethoxylation resulting in increased production of phenol and catechol.<sup>53</sup> The percentage area of 2-methoxy-phenol (guaiacol) increased with temperatures up to 600 °C (exp. IV); this percentage decreased above this temperature (exp. V). This can be explained by the fact that high temperatures can lead to new radical reactions to produce alkylated phenolic monomers.<sup>54</sup>

The presence of significant amounts of phenolic compounds in the bio-oil is extremely relevant because it becomes an alternative to phenol that is derived from fossil fuels in phenolic resins, which are used to produce chemical products such as detergents, phenolic herbicides, pharmaceuticals, antioxidants, and synthetic bioplastics.<sup>54</sup> Catechols were the major phenol compound in the bean pod bio-oil. Mabrouk *et al.*,<sup>55</sup> studied the valorization of the lignin fraction present in lignocellulosic biomass due to the presence of phenols. These compounds are important for the chemical industry in the production of resin formulations.

The existence of sugars in bio-oils, such as levoglucosan, can be explained by the breakage and rearrangement of chemical bonds in the cellulose molecule while nitrogen compounds belonging to the group of amines are typical products of the degradation of proteins contained in bean pods.<sup>40</sup>

In general, the bean pod bio-oils presented similarities in their composition, with compounds that were similar to those detected by Saikia *et al.*,<sup>56</sup> in the bio-oil obtained from the pyrolysis of *Ipomoea carnea*. The present compounds

belong to the classes of phenols and their derivatives, acids, esters, alcohols, and various aromatics, furans, and ketones. In addition, Aziz *et al.*,<sup>44</sup> performed pyrolysis in palm kernel shell (PK), wood chips (WC), and sago wastes (SW) and identified that most of the compounds present in the bio-oils were phenolics (phenol, guaiacol, cresol, catechol, syringol, and eugenol), carboxylic acids (propanoic, palmitic, oleic, and stearic), ketones, aldehydes, esters, and sugars (levoglucosan).

## Conclusions

The physicochemical characterization of the biomass was of paramount importance to define the pyrolysis temperature to be used because it directly influences the cracking process and the chemical composition of the bio-oil. The results showed that the bean pod presented moisture content below 10% and high carbon (42.01%) and oxygen (46.36%) contents. The superior calorific power of the bean pod (17.55 MJ kg<sup>-1</sup>) was considered satisfactory for its use as biomass. These results confirmed the potential of bean pods in thermochemical processes such as pyrolysis. Although the pyrolysis conditions did not reflect on qualitative differences in the composition of the studied bio-oils, the phenol class predominant in these bio-oils, represents an excellent potential for the production of guaiacols and catechols for use in the chemical industry. Hence, our studies showed the potential of bean pod bio-oils as a source of commercially valuable chemicals represented by the presence of phenolic compounds such as 2-methoxy-phenol (guaiacol), 3-methyl-1,2-benzenediol (3-methyl catechol), phenol, 4-hydroxybenzaldehyde, and 1,2-benzenediol (pyrocatechol) among others.

## Supplementary Information

Supplementary information is available free of charge at <http://jbc.ssbq.org.br> as PDF file.

## Acknowledgments

This study was financially supported by the Conselho Nacional de Pesquisa (CNPq), Coordenação de Aperfeiçoamento de Pessoal de Nível Superior- Brasil (CAPES)-Finance code 424863/2018-9 and 310980/2018-6, and Fundação de Apoio à Pesquisa e a Inovação Tecnológica do Estado de Sergipe (FAPITEC/SE). The authors are particularly thankful to CLQM-Centro de Laboratórios de Química Multiusuários, for analytics support.

## Author Contributions

Roberta M. Santos was responsible for conceptualization, formal analysis, investigation, writing original; Diego F. Bispo for formal analysis; Honnara S. Granja for formal analysis; Eliane M. Sussuchi for resources; André Luis D. Ramos for supervision and Lisiane S. Freitas for conceptualization, resources, funding acquisition, writing review and editing.

## References

- Garcia, R.; Pizarro, C.; Lavin, A. G.; Bueno, J. L.; *Fuel* **2017**, *195*, 182.
- Faria, M. A.; Araújo, A.; Pinto, E.; Oliveira, C.; Olívia-Teles, M. T.; Almeida, A.; Delerue- Matos, C.; Ferreira, I. M. P. L. V. O.; *J. Funct. Foods* **2018**, *50*, 201.
- Chagas, E.; Araújo, A. P.; Teixeira, M. G.; Guerra, J. G. M.; *Rev. Bras. Cienc. Solo* **2007**, *31*, 723.
- Welfle, A.; *Biomass Bioenergy* **2017**, *105*, 83.
- Wang, S.; Dai, G.; Yang, H.; Luo, Z.; *Prog. Energy Combust. Sci.* **2017**, *62*, 33.
- Ma, H.; Li, H.; Zhao, W.; Li, X.; Long, J.; *Energy Procedia* **2019**, *158*, 375.
- Gumisiriza, R.; Hawumba, J. F.; Okure, M.; Hensel, O.; *Biotechnol. Biofuels* **2017**, *10*, DOI: 10.1186/s13068-016-0689-5.
- Mythili, R.; Venkatachalam, P.; Subramanian, P.; Uma, D.; *Bioresour. Technol.* **2013**, *138*, 71.
- Hawash, S. I.; Farah, J. Y.; El-Diwani, G.; *J. Anal. Appl. Pyrolysis* **2017**, *124*, 369.
- Silva, K. J. D.; Rocha, M. M.; Menezes Jr., J. A. N. In *A Cultura do Feijão-Caupi no Brasil*; Embrapa: Teresina, 2016, p. 68.
- Neto, M. C.; Bartels, P. G.; *Veg. Rep.* **1992**, *12*, 167.
- ASTM D3173-87: *Standard Test Method for Moisture in the Analysis Sample of Coal and Coke*, Philadelphia, 1996.
- ASTM D3174-89: *Standard Test Method for Ash in the Analysis Sample of Coal and Coke from Coal*, Philadelphia, 1989a.
- ASTM D1762-84: *Standard Test Method for Chemical Analysis of Wood Charcoal*, Philadelphia, 1990.
- Sheng, C.; Azevedo, J. L. T.; *Biomass Bioenergy* **2005**, *28*, 499.
- Hames, B.; Scarlata, C.; Sluiter, A.; NREL/TP-510-42625: *Determination of Protein Content in Biomass*; National Renewable Energy Laboratory: Golden, USA, 2008.
- Van Soest, P. J.; *J. Anim. Sci.* **1967**, *26*, 119.
- Onorevoli, B.; Machado, M. E.; Dariva, C.; Franceschi, E.; Krause, L. C.; Jacques, A. R. A.; Caramão, E. B.; *Ind. Crops Prod.* **2014**, *52*, 8.
- Santos, R. M.; Santos, A. O.; Sussuchi, E. M.; Nascimento, J. S.; Lima, A. S.; Freitas, L. S.; *Bioresour. Technol.* **2015**, *196*, 43.
- Bridgwater, A. V.; *Biomass Bioenergy* **2012**, *38*, 68.
- Wilson, D. M.; Dalluge, D. L.; Rover, M.; Heaton, E. A.; Brown, R. C.; *Bioenergy Res.* **2013**, *6*, 103.
- Yildiz, G.; Ronsse, F.; Venderbosch, R.; van Duren, R.; Kersten, S. R. A.; Prins, W.; *Appl. Catal., B* **2015**, *168*, 203.
- Biswas, B.; Pandey, N.; Bisht, Y.; Singh, R.; Kumar, J.; Bhaskar, T.; *Bioresour. Technol.* **2017**, *237*, 57.
- Tanger, P.; Field, J. L.; Jahn, C. E.; DeFoort, M. W.; Leach, J. E.; *Front. Plant Sci.* **2013**, *4*, 218.
- Cai, J.; He, Y.; Yu, X.; Banks, S. W.; Yang, Y.; Zhang, X.; Yu, Y.; Liu, R.; Bridgwater, A. V.; *Renewable Sustainable Energy Rev.* **2017**, *76*, 309.
- Ozyuguran, A.; Akturk, A.; Yaman, S.; *Fuel* **2018**, *214*, 640.
- Park, Y. K.; Yoo, M. L.; Lee, H. W.; Park, S. H.; Jung, S. C.; Park, S. S.; Kim, S. C.; *Renewable Energy* **2012**, *42*, 125.
- Lo, S.-L.; Huang, Y.-F.; Chiueh, P.-T.; Kuan, W.-H.; *Energy Procedia* **2017**, *105*, 41.
- Ho, D. P.; Ngo, H. H.; Guo, W.; *Bioresour. Technol.* **2014**, *169*, 742.
- Kan, T.; Strezov, S. V.; Evans, T. J.; *Renewable Sustainable Energy Rev.* **2016**, *57*, 1126.
- Dong, C.; Zhang, Z.; Lu, Q.; Yang, Y.; *Energy Convers. Manage.* **2012**, *57*, 49.
- Bensidhom, G.; Hassen-Trabelsi, A. B.; Alper, K.; Sghairoun, M.; Zaafouri, K.; Trabelsi, I.; *Bioresour. Technol.* **2018**, *247*, 363.
- Raj, T.; Kapoor, M.; Gaur, R.; Christopher, J.; Lamba, B.; Tuli, D. K.; Kumar, R.; *Energy Fuels* **2015**, *29*, 3111.
- Kok, M. V.; Ozgur, E.; *Fuel Process. Technol.* **2013**, *106*, 739.
- Mishra, R. K.; *Bioresour. Technol.* **2018**, *251*, 63.
- Sindhu, R.; Kuttiraja, M.; Binod, P.; Sukumaran, R. K.; Pandey, A.; *Renew. Energy* **2014**, *62*, 362.
- Huang, X. X.; Cao, J. P.; Zhao, X. Y.; Wang, J. X.; Fan, X.; Zhao, Y. P.; Wei, X. Y.; *Fuel* **2016**, *169*, 93.

38. Pereira, S. C.; Maehara, L.; Machado, C. M. M.; Farinas, C.; *Renewable Energy* **2016**, *87*, 607.
39. Akhtar, J.; Amin, N. S.; *Renewable Sustainable Energy Rev.* **2012**, *16*, 5101.
40. Guedes, R. E.; Luna, A. S.; Torres, A. R.; *J. Anal. Appl. Pyrolysis* **2018**, *129*, 134.
41. Charusiri, W.; Vitidsant, T.; *Sustainable Chem. Pharm.* **2018**, *10*, 71.
42. Dhyan, V.; Bhaskar, T.; *Renewable Energy* **2018**, *129*, 695.
43. Aboulkas, A.; Hammani, H.; El Achaby, M.; Bilal, E.; Barakat, A.; El Harfi, K.; *Bioresour. Technol.* **2017**, *243*, 400.
44. Aziz, S. M. A.; Wah, R.; Ngaini, Z.; Hamdan, S.; *Fuel Process. Technol.* **2013**, *106*, 744.
45. Demirbas, A.; Al-Ghamdi, K.; *Pet. Sci. Technol.* **2015**, *33*, 732.
46. Fan, Y.; Cai, Y.; Li, X.; Yin, H.; Yu, N.; Zhang, R.; Zhao, W.; *J. Anal. Appl. Pyrolysis* **2014**, *106*, 63.
47. Xiong, Z.; Wang, Y.; Syed-Hassan, S. S. A.; Hu, X.; Han, H.; Su, S.; Xu, K.; Jiang, L.; Guo, J.; Berthold, E. E. S.; Hu, S.; Xiang, J.; *Energy Convers. Manage.* **2018**, *163*, 420.
48. Stas, M.; Kubicka, D.; Chudoba, J.; Pospisil, M.; *Energy Fuels* **2014**, *28*, 385.
49. Mantilla, S. V.; Manrique, A. M.; Gauthier-Maradei, P.; *Waste Biomass Valorization* **2015**, *6*, 371.
50. Hosoya, T.; Kawamoto, H.; Saka, S.; *J. Anal. Appl. Pyrolysis* **2007**, *80*, 118.
51. Wu, Y.; Wu, S.; Zhang, H.; Xiao, R.; *Fuel Process. Technol.* **2018**, *179*, 436.
52. Fan, L.; Zhang, Y.; Liu, S.; Zhou, N.; Chen, P.; Cheng, Y.; Addy, M.; Lu, Q.; Omar, M. M.; Liu, Y.; Wang, Y.; Dai, L.; Anderson, E.; Peng, P.; Lei, H.; Ruan, R.; *Bioresour. Technol.* **2017**, *241*, 1118.
53. Jung, K. A.; Nam, C. W.; Woo, S. H.; Park, J. M.; *J. Anal. Appl. Pyrolysis* **2016**, *120*, 409.
54. Naik, D. K.; Monika, K.; Prabhakar, S.; Parthasarathy, R.; Satyavathi, B.; *J. Therm. Anal. Calorim.* **2017**, *127*, 1277.
55. Mabrouk, A.; Erdocia, X.; Alriols, M. G.; Labidi, J.; *J. Cleaner Prod.* **2018**, *198*, 142.
56. Saikia, P.; Gupta, U. N.; Barman, R. S.; Katak, R.; Chutia, R. S.; Baruah, B. P.; *Bioenergy Res.* **2015**, *8*, 1212.

Submitted: September 9, 2019

Published online: December 20, 2019

